

CFA/VISHNO 2016

**Absorption quasi-parfaite du son par un métamatériau
acoustique suite à l'accumulation de résonances due à une
propagation lente**

N. Jimenez, W. Huang, J.-P. Groby, V. Romero García et V. Pagneux
Laboratoire d'Acoustique de l'Université du Maine, Avenue Olivier Messiaen, Cedex9,
72085 Le Mans, France
noe.jimenez@univ-lemans.fr



LE MANS

La propagation du son dans un metamatériau acoustique constitué d'un réseau unidimensionnel de fentes minces chargées par des résonateurs de Helmholtz est étudiée. Un modèle analytique est présenté, dont la limite asymptotique basses fréquences permet de déterminer les paramètres effectifs du metamatériau acoustique. La relation de dispersion dans la fente est modifiée par la présence des résonateurs dans le régime basses fréquences. La vitesse de propagation dans celle-ci est drastiquement réduite et par conséquent une propagation lente du son est observée. L'effet principal de cette propagation anormale est une accumulation des résonances à la borne inférieure de la bande interdite due à la résonance de Helmholtz. Chaque résonance correspond à une paire zéro/pôle des valeurs propres de la matrice de diffusion représentée dans le plan de fréquences complexes. Ces zéros et pôles sont conjugués l'un de l'autre et par conséquent symétriques par rapport à l'axe de fréquences réelles dans le cas sans perte. Une fois les pertes du système introduites, les zéros des valeurs propres symétriques et antisymétriques se rapprochent de l'axe des fréquences réelles, de façon à ce que pour une des résonances les zéros des valeurs propres symétrique et antisymétrique soient proches de l'axe de fréquences réelles. Cela se traduit notamment par une réduction importante et simultanée de la réflexion et de la transmission du système, c'est-à-dire une absorption quasi-parfaite pour cette fréquence dans un système sublongueur d'onde.

1 Introduction

The acoustic absorption of low frequency sound with sub-wavelength panels is of particular interest because traditional absorbers, e.g. porous media, requires structures of the order of the wavelength and, therefore, are not practical for commercial and industrial applications. Other typical low-frequency absorbers include perforated panels of simply resonant plates, but commonly the maximum absorption achieved is limited.

On the other hand, perfect absorption (PA) is of particular interest for many applications such as energy conversion [1], time reversal technology [2], coherent perfect absorbers [3] or soundproofing [4] among others. For absorption application it is desirable to avoid bulky structures and design sub-wavelength structures. The recent advances in PA have motivated an increasing interest on the design of perfect absorbers which at the same time are sub-wavelength structures. Recently in acoustics, impedance matched sub-wavelength membranes [5] with broadband perfect absorption [6], quarter-wavelength resonators [7], unidirectional nearly perfect absorption systems based on Helmholtz resonator [8] have been shown as sub-wavelength perfect absorbers.

In this work, we present the design of sub-wavelength transparent panels considering reflection and transmission with the coupling between the exterior medium, i.e., considering the real leakage of the resonant building blocks of the structure. We consider flat vertical panels perforated with slits and Helmholtz resonators (HRs). The inclusion of HRs induces creates a band-gap at its resonant frequency, inducing slow-sound conditions in the slit. Therefore, strong absorption can be achieved at the collective modes of the HRs. The present work explores the limits of PA achieved by these sub-wavelength transparent panels.

2 Theoretical models

We consider a flat vertical panel of thickness L perforated with open slits of height h separated a distance d , as shown in Fig. 1. A periodic array of a rectangular cross-section Helmholtz resonators (HRs) was placed in the top of the slits following a square lattice of step a . The wall boundary conditions was assumed to be perfectly rigid. Thermo-viscous losses were included in the slits and the ducts that compose the Helmholtz resonators by its complex

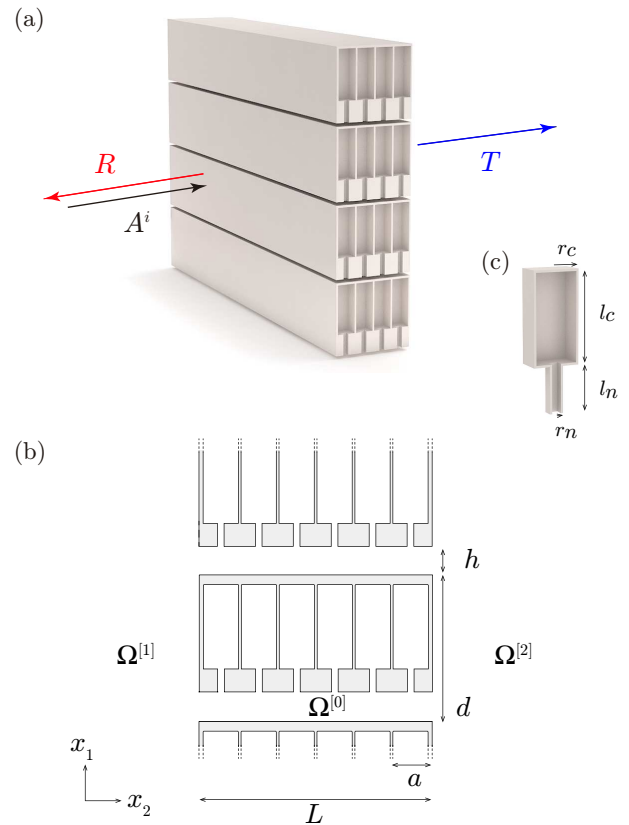


FIGURE 1 – (a) Conceptual view of the panel and (b) Helmholtz resonator. (c) Scheme of the slitted panel.

and frequency dependent density and bulk modulus [9]. The HRs impedance, Z_{HR} , was calculated accounting for the end corrections at the neck-slit and neck-cavity boundaries [10].

A modal expansion method was developed to represent the field on each $\Omega^{[i]}$ domain, where the effect of the resonators is accounted by a continuous effective impedance at the wall of the slit, given by $Z_i = Z_{HRs}/\phi_n$ with $\phi_n = S_n/a^2$ the slit porosity where S_n is the cross section of the neck. Assuming the continuity of pressure between domains, and considering perfectly rigid boundary conditions for the walls, the reflection, R , and transmission, T , coefficients can be obtained by solving the mode-matching system.

In the low frequency regime, the effective wavenumber inside the slits of the panel is

$$k_e = k_2^{[1]} = \sqrt{k_1^2 - k_{10}^2} \quad (1)$$

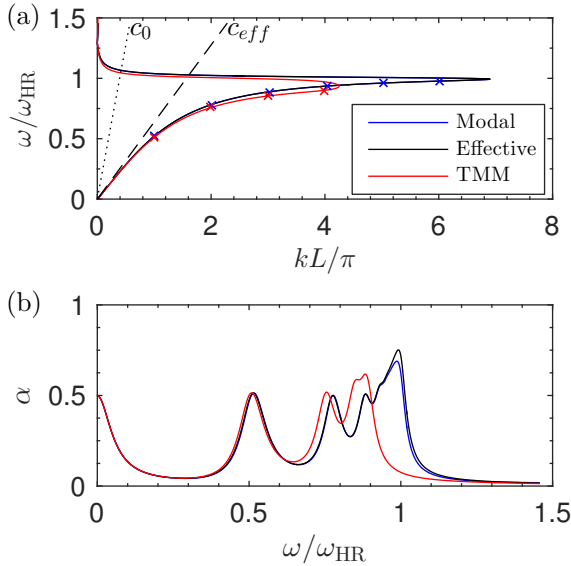


FIGURE 2 – (a) Dispersion relation in the slit using (red) TMM, (blue) full modal expansion and (black) effective parameters. (b) corresponding attenuation.

with

$$k_{10} = 1/h \sqrt{-i\omega\rho_s h/Z_1} \quad (2)$$

the transversal component of the wavenumber. Then, using the Helmholtz resonator impedance, $Z_1 = Z_{HR}/\phi_n$, the complex and frequency dependent effective density and bulk modulus of the slit become

$$\rho_e = \frac{\rho_s}{\phi} \quad (3)$$

and

$$K_e = K_s \left[\phi \left(1 + \frac{K_s(S_c l_c K_n + S_n l_n K_c)\phi_n}{K_n(S_n K_c - l_n S_c l_c \rho_n \omega^2)h} \right) \right]^{-1}, \quad (4)$$

where S_i and l_i are the surface and length of the i element of the resonator, the subscript s , n and c denotes the slit, neck and cavity of the HRs and the total porosity $\phi = h/d$. In the lossless case, $K_n = K_c = K_{air}$ and $\rho_n = \rho_c = \rho_{air}$, therefore, the low frequency branch of the phase speed can be expressed as $c_{eff} = c_a / \sqrt{1 + V_{tot}\phi_n/hS_n}$. The use of effective parameters allows the calculation of reflection and transmission coefficients, and finally, the absorption of the system as $\alpha = 1 - |T|^2 - |R|^2$.

The full modal calculation and its low frequency approximation assumes a wall impedance at the interior faces of the slits, leading to an infinite number of resonances in the slow sound regime. However, in reality the number of resonances is effectively $N - 1$, being N the number of resonators in the slit, imposing limitations to the application of slow sound for designing acoustic absorbing systems [10]. Therefore, a discrete model is developed accounting for the finite number of resonators using the Transfer Matrix Method (TMM) [10], in which the end correction is included for accounting for the radiation of the periodic arrangement of slits.

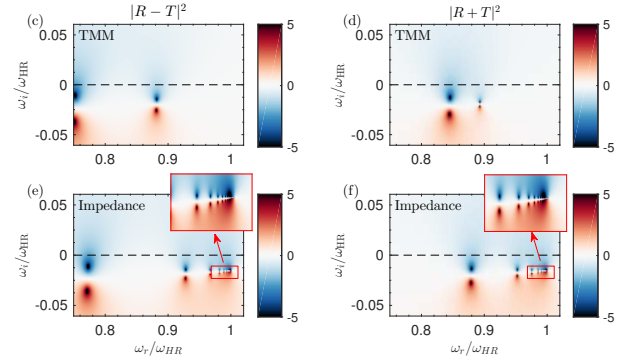


FIGURE 3 – (c-f) Complex frequency plane of the symmetric and anti-symmetric scattering matrix for the TMM method and impedance model (effective parameters).

3 Results

3.1 Purely periodic structures

Figure 3 summarizes the results for a panel with $N = 6$ equally sized resonators. The dispersion relation in the interior of the slit is shown in Fig. 3 (a). It can be noticed how when resonators are included an hybridization band-gap is generated at the resonance frequency of the HRs. Therefore, in the first band slow sound conditions are achieved, where the asymptotic value given by c_{eff} is observed in the low frequency regime. Furthermore, for frequencies just below the band gap extremely slow sound is observed, where sound absorption can be achieved at the induced resonant frequencies $kL/\pi = 1, 2, \dots$. In addition, important differences are observed between the calculation with impedance models and using TMM. The full modal expansion, red curve in Fig. 3 (a), assumes a continuum wall impedance, $Z_1 = Z_{HRs}/\phi$, and therefore, the effect of the finite number of resonators is not included. In contrast, this effect is accounted by TMM, blue curve in Fig. 3 (a). The result of including N resonators is that the number of possible low-frequency resonances is limited to $N - 1$, which are in fact the possible collective modes of the HRs [10].

A more clear view of this phenomena can be observed in the complex frequency plane representation of the transmission and reflection matrix. Figure 3 (c-f) shows the quantities $|R - T|^2$ and $|R + T|^2$ corresponding to the zero-pole structure of the symmetric and anti-symmetric problem respectively. First, it can be observed that the zero-pole structure for the impedance model, Fig. 3 (e-f), presents an infinite collection of zeros and poles that are stretched around ω_{HR} . By contrast, the corresponding structure obtained by TMM, Fig. 3 (c-d), the number of zeros/poles is limited to $N - 1$. Secondly, it can be observed that the zeros of the symmetric problem, ω_{sym}^Z , are located at frequencies staggered to the zeros of the anti-symmetric ω_{asym}^Z . It is worth noting here that perfect absorption can only be achieved if both, the symmetric and antisymmetric zeros for a given frequency are located in the real axis, $\text{Im}(\omega_{sym}^Z) = \text{Im}(\omega_{asym}^Z) = 0$, i.e. the zeros of the symmetric and antisymmetric problem must be critically coupled. As the zero-pole structure is staggered in frequency, perfect critical coupling is not possible. However quasi-perfect absorption can be achieved. If a single zero is placed in the real axis, then the absorption of the system is $\alpha > 0.5$. However, as zeros present some frequency-width, the

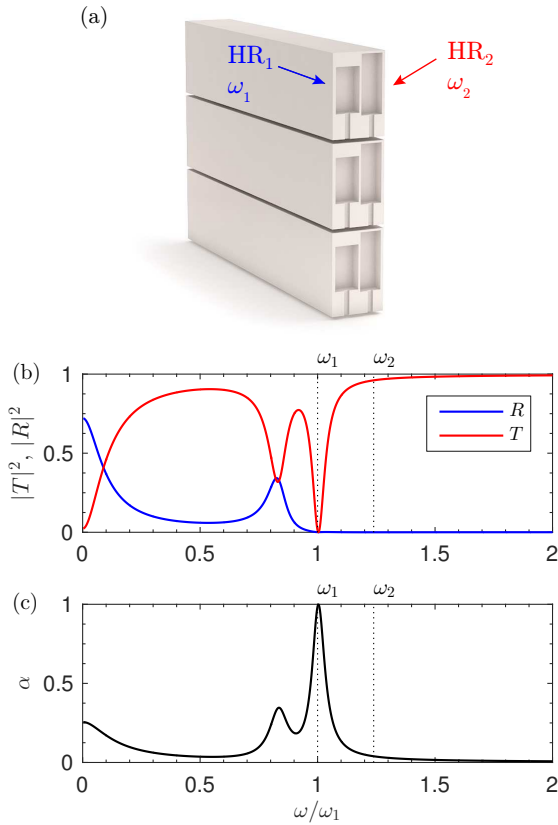


FIGURE 4 – (a) View of the perfect sub-wavelength absorbing panel.(b) Transmission and reflection using TMM, (c) absorption.

system properties can be tuned for place a zero of the anti-symmetric (symmetric) problem as close as possible to the corresponding symmetric (anti-symmetric) one and, simultaneously, both as close as possible to the real axis.

3.2 Critical coupling by symmetry breaking

One way to break the symmetry and unstagger the zero-pole structure is to include HRs of different resonant frequencies [8]. This situation is presented in Fig. 4. In Fig. 4 (a-b) the dotted lines indicates the position of the resonances for $N = 2$ resonators. In this conditions, the high frequency resonator acts as a rigid wall and as it can be observed in Fig. 4 (a) the transmission is forbidden at band-gap frequencies. Then, the parameters of the lower frequency resonator can be tuned for include the exact losses necessary to reduce the reflection. In the complex frequency plane, this reduces to place both zeros of the symmetric ($R - T$) and anti-symmetric ($R + T$) in the real axis as shown in Fig. 5 (d-e). The absorption of the sample reaches $\alpha = 1$ for a sample of thickness $L/\lambda_0 = 26$ with λ_0 the wavelength in air at the resonant frequency.

4 Conclusion

The limits of acoustic absorption in sub-wavelength transparent panels using slow sound are discussed. The current work shows that as long the Zero-Pole structure of the symmetric and anti-symmetric problems is staggered, no perfect absorption is possible using regular arrays of resonant elements in a cavity. We show that using different

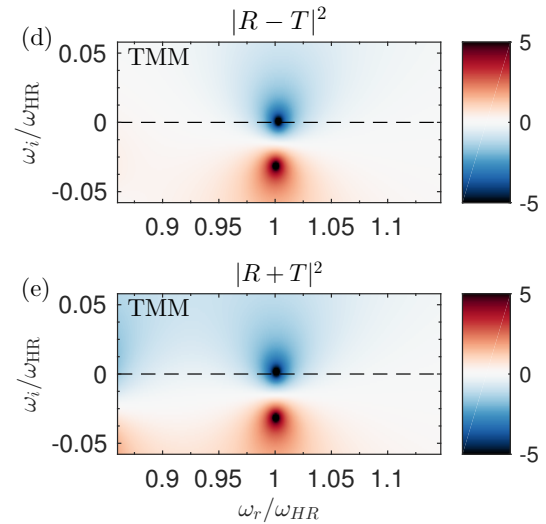


FIGURE 5 – (d-e) complex frequency plane of the symmetric and anti-symmetric scattering matrix.

resonators the symmetry can be broken and therefore perfect absorption by critical coupling is achieved for sub-wavelength thickness transparent panels.

Acknowledgement

This work has been funded by the Metaudible project ANR-13-BS09-0003, co-funded by ANR and FRAE.

Références

- [1] Law, M., Greene, L., Johnson, J., Saykally, R. and Yang, P. "Nanowire dye-sensitized solar cells," *Nat. Mater.*, vol. 4, p. 455 (2005).
- [2] Derode, A., Roux, P., Fink, M.. "Robust acoustic time reversal with high-order multiple scattering," *Phys. Rev. Lett.*, vol. 75, p. 4206, (1995).
- [3] Chong, Y., Ge, L., Cao, H., Stone, A. "Coherent perfect absorbers : Time-reversed lasers," *Phys. Rev. Lett.*, vol. 105, p. 053901, (2010).
- [4] Mei, J. *et al.* "Dark acoustic metamaterials as super absorbers for low-frequency sound," *Nature Communications*, vol. 3, p. 756, (2012).
- [5] Ma, G., Yang, M., Xiao, S., Yang, Z. and Sheng, P. "Acoustic metasurface with hybrid resonances," *Nature Mater.*, vol. 13, p. 873, (2014).
- [6] Romero-García, V., Theocharis, G., Richoux, O., Merkel, A., Tournat, V., and Pagneux, V. "Perfect and broadband acoustic absorption by critically coupled sub-wavelength resonators," *Sci. Rep.*, vol. 6, p. 19519 (2016).
- [7] Groby, J. P., Huang, W., Lardeau, A., and Aurégan, Y., "Use of slow wave to design simple sound absorbing metamaterials," *J. App. Phys*, vol. 117, p. 124903 (2015).
- [8] A. Merkel, G. Theocharis, O. Richoux, V. Romero-García, and V. Pagneux. Control of acoustic absorption in one-dimensional scattering by resonant scatterers. *Appl. Phys. Lett.*, 107(24) :244102, 2015.
- [9] M. R. Stinson. The propagation of plane sound waves in narrow and wide circular tubes, and generalization

- to uniform tubes of arbitrary cross-sectional shape. *J. Acoust. Soc. Am.*, 89(2) :550–558, 1991.
- [10] G. Theocharis, O. Richoux, V. R. García, A. Merkel, and V. Tournat. Limits of slow sound propagation and transparency in lossy, locally resonant periodic structures. *New J. Phys.*, 16(9) :093017, 2014.